HAL
open science

Concavity of the collective excitation branch of a Fermi gas in the BEC-BCS crossover

H Kurkjian, Yvan Castin, A Sinatra

To cite this version:

H Kurkjian, Yvan Castin, A Sinatra. Concavity of the collective excitation branch of a Fermi gas in the BEC-BCS crossover. Physical Review A : Atomic, molecular, and optical physics [1990-2015], 2016, 93, pp.013623. 10.1103/PhysRevA.93.013623 . hal-01228798v2

HAL Id: hal-01228798

https://hal.science/hal-01228798v2

Submitted on 26 Jan 2016

HAL is a multi-disciplinary open access archive for the deposit and dissemination of scientific research documents, whether they are published or not. The documents may come from teaching and research institutions in France or abroad, or from public or private research centers.

L'archive ouverte pluridisciplinaire **HAL**, est destinée au dépôt et à la diffusion de documents scientifiques de niveau recherche, publiés ou non, émanant des établissements d'enseignement et de recherche français ou étrangers, des laboratoires publics ou privés.

Concavity of the collective excitation branch of a Fermi gas in the BEC-BCS crossover

H. Kurkjian, Y. Castin, A. Sinatra
Laboratoire Kastler Brossel, ENS, PSL, CNRS, UPMC-Sorbonne Universités and Collège de France, Paris, France

We study the concavity of the dispersion relation $q \mapsto \omega_{\mathbf{q}}$ of the bosonic excitations of a three-dimensional spin-1/2 unpolarized Fermi gas in the Random Phase Approximation (RPA). In the limit of small wave numbers q we obtain analytically the spectrum up to order 5 in q. In the neighborhood of $q = 0$, a change in concavity between the convex Bose-Einstein condensation (BEC) limit and the concave BCS limit takes place at $\Delta/\mu \simeq 0.869$ $[1/(k_F a) \simeq -0.144]$, where a is the scattering length between opposite spin fermions, k_F is the Fermi wave number and Δ the gap according to BCS theory, and μ is the chemical potential. At that point the branch is concave due to a negative fifth order term. Our results are supplemented by a numerical study that shows the border between the zone of the (q, Δ) plane where $q \mapsto \omega_{\mathbf{q}}$ is concave and the zone where it is convex.

PACS numbers: 03.75.Kk, 67.85.Lm, 47.37.+q

I. INTRODUCTION

Cold atomic gases offer a broad flexibility of the microscopic parameters in exploring the many-body problem. In particular, in spin-1/2 Fermi gases, the interaction strength can be adjusted experimentally using Feshbach resonances without inducing strong three-body losses. This degree of freedom, unique among Fermi systems, allowed cold-atom experiments [1–9] to study the crossover between a superfluid of Cooper pairs in the so-called Bardeen-Cooper-Schrieffer (BCS) regime of interaction and a superfluid of tightly bound, almost bosonic, dimers in the Bose-Einstein Condensation (BEC) regime. Another advantage of cold atomic gases is the simple theoretical description of the interactions that the cold and dilute regime in which they occur allows for. For a Fermi gas in two spin states $\uparrow$ and $\downarrow$, one can show that the only significant interactions at low temperature and weak density occur between opposite spins fermions in the s wave and can be fully characterized by a single parameter called the scattering length and denoted by a. In this propitious theoretical framework, entirely analytical studies of experimentally accessible properties of the gas are possible. This article is one of those.

At zero temperature, the three-dimensional spatially homogeneous unpolarized Fermi gas is fully paired and its excitation spectrum consists of two branches: a fermionic branch of excitation of the internal degrees of freedom of the $\uparrow\downarrow$ pairs of fermions and a bosonic branch of excitation of their center-of-mass motion, which has a phononic behavior in the long wavelength limit. The latter branch is sometimes said to be collective since it involves a large number of the fermionic modes of internal excitations of the pairs. The fermionic branch is described to lowest order by the BCS theory. To tackle the bosonic branch several approaches have been proposed: The Random Phase Approximation (RPA) of Anderson [10], a Gaussian approximation of the action in a path integral framework [11, 12], a Green's function approach associated with a diagrammatic approximation [13], and a linearization of the time dependent BCS variational equations [14]. Remarkably, those theories all lead to the same approximate spectrum of bosonic excitations, which they describe by the same implicit equation.

The concavity of this spectrum has been studied in the weak-coupling BCS limit [11] and, in a qualitative way, in the rest of the BEC-BCS crossover [13, 15, 16]. A complete quantitative study is thus missing, a gap that this article intends to bridge. In particular, we obtain the spectrum analytically up to order 5 in the wave number q of the center of mass of the pairs. This allows us to conclude on the concavity of the branch of excitation in a neighborhood of $q = 0$ over the whole BEC-BCS crossover.

Several physically relevant problems can be addressed after our study. First, the processes that dominate the collective mode damping at low temperature can be identified. If the branch is convex over a neighborhood of $q = 0$ then the Landau-Beliaev 2 phonons $\leftrightarrow$ 1 phonon interaction processes [17, 18] dominate while if it is concave, those processes are forbidden by momentum and energy conservation and the Landau-Khalatnikov 2 phonons $\leftrightarrow$ 2 phonons processes [19] take over. At low temperature the contribution of the gapped fermionic branch to the collective mode damping is exponentially small [20]. Second, the quantitative knowledge of the concavity parameter γ is required in order to predict the phonon damping rate due to the 2 phonons $\leftrightarrow$ 1 phonon processes in the convex case beyond the quantum hydrodynamics approximation [16], or due to the 2 phonons $\leftrightarrow$ 2 phonons processes in the concave case where the effective interaction predicted by quantum hydrodynamics involves virtual 2 phonons $\leftrightarrow$ 1 phonon processes and depends on γ. Finally, the knowledge of γ gives access to the phase diffusion coefficient of the condensate of pairs, a quantity responsible for an intrinsic and fundamental limit to the coherence time of the gas [14].

II. THE RPA EQUATION ON THE EXCITATION SPECTRUM

The RPA equation yielding implicitly the energy $\hbar\omega_{\mathbf{q}}$ of the collective excitations as a function of their wave vector $\mathbf{q}$ is

$$I_{++}(\omega_{\mathbf{q}},q)I_{--}(\omega_{\mathbf{q}},q)=\hbar^2\omega_{\mathbf{q}}^2\left[I_{+-}(\omega_{\mathbf{q}},q)\right]^2. \quad (1)$$

The collective nature of the bosonic modes is visible in the quantities $I_{\sigma\sigma'}$ which are integrals on the relative wave vector $\mathbf{k}$ of the pairs and depend on $\omega_{\mathbf{q}}^2$ *via* the denominator of their integrand [13]:

$$I_{++}(\omega,q) = \int \mathrm{d}^3k\left[\frac{(\epsilon_{\mathbf{k+q}/2}+\epsilon_{\mathbf{k-q}/2})(U_{\mathbf{k+q}/2}U_{\mathbf{k-q}/2}+V_{\mathbf{k+q}/2}V_{\mathbf{k-q}/2})^2}{\hbar^2\omega^2-(\epsilon_{\mathbf{k+q}/2}+\epsilon_{\mathbf{k-q}/2})^2}+\frac{1}{2\epsilon_{\mathbf{k}}}\right], \quad (2)$$

$$I_{--}(\omega,q) = \int \mathrm{d}^3k\left[\frac{(\epsilon_{\mathbf{k+q}/2}+\epsilon_{\mathbf{k-q}/2})(U_{\mathbf{k+q}/2}U_{\mathbf{k-q}/2}-V_{\mathbf{k+q}/2}V_{\mathbf{k-q}/2})^2}{\hbar^2\omega^2-(\epsilon_{\mathbf{k+q}/2}+\epsilon_{\mathbf{k-q}/2})^2}+\frac{1}{2\epsilon_{\mathbf{k}}}\right], \quad (3)$$

$$I_{+-}(\omega,q) = \int \mathrm{d}^3k\frac{(U_{\mathbf{k+q}/2}U_{\mathbf{k-q}/2}+V_{\mathbf{k+q}/2}V_{\mathbf{k-q}/2})(U_{\mathbf{k+q}/2}U_{\mathbf{k-q}/2}-V_{\mathbf{k+q}/2}V_{\mathbf{k-q}/2})}{\hbar^2\omega^2-(\epsilon_{\mathbf{k+q}/2}+\epsilon_{\mathbf{k-q}/2})^2}. \quad (4)$$

We have introduced the amplitudes $U_{\mathbf{k}}$ and $V_{\mathbf{k}}$ and the eigenenergies $\epsilon_{\mathbf{k}}$ of the fermionic eigenmodes of the BCS theory [21]:

$$\epsilon_{\mathbf{k}} = \sqrt{\left(\frac{\hbar^2k^2}{2m}-\mu\right)^2+\Delta^2}, \quad (5)$$

$$U_{\mathbf{k}} = \sqrt{\frac{1}{2}\left(1+\frac{\frac{\hbar^2k^2}{2m}-\mu}{\epsilon_{\mathbf{k}}}\right)}, \quad (6)$$

$$V_{\mathbf{k}} = \sqrt{\frac{1}{2}\left(1-\frac{\frac{\hbar^2k^2}{2m}-\mu}{\epsilon_{\mathbf{k}}}\right)}, \quad (7)$$

where m is the mass of a fermion. The two natural parameters of the BCS theory, with which we express the energy $\hbar\omega_{\mathbf{q}}$, are the chemical potential μ, identical for the two spin states, and Δ, the gap in the BCS spectrum of the fermionic excitations when μ is positive. If needed, they can be replaced by the scattering length a and the total density ρ of the gas by inverting the two following relations [22, 23]:

$$\frac{m}{4\pi\hbar^2a} = \int\frac{d^3k}{(2\pi)^3}\left(\frac{m}{\hbar^2k^2}-\frac{1}{2\epsilon_{\mathbf{k}}}\right), \quad (8)$$

$$\rho = \int\frac{d^3k}{(2\pi)^3}2|V_{\mathbf{k}}|^2. \quad (9)$$

In practice, the Fermi wave number k_F defined by $\rho = k_F^3/(6\pi^2)$ is often used instead of the density.

III. GLOBAL NUMERICAL STUDY OF THE CONCAVITY

From a numerical solution of the dispersion equation (1) we obtain the dispersion relation $q\mapsto\omega_{\mathbf{q}}$ over its existence domain. We show an example in Figure 1 in the unitary limit $1/(k_Fa)=0$, where $\Delta/\mu\simeq 1.162$ according to the BCS theory. Rather than $q\mapsto\omega_{\mathbf{q}}$ itself, we plot as a black solid line the function $q\mapsto\omega_{\mathbf{q}}-cq$, where c is the speed of sound and $q\mapsto cq$ is the linear part of the spectrum. The concavity properties of this function are the same as those of $q\mapsto\omega_{\mathbf{q}}$, but they are more visible graphically at low q, because they are not masked by the dominant linear part, which anyway plays no role in the selection of the damping processes mentioned at the end of the Introduction. In the figure, it is apparent that the dispersion relation exhibits an inflection point at $q/k_\mu\simeq 0.795$, where $k_\mu=(2m\mu)^{1/2}/\hbar$, separating a low-$q$ interval over which the dispersion relation is convex and a high-q interval over which it is concave. As a consequence, according to the RPA, the leading damping processes of the collective excitations of the unitary gas at low temperature are the Beliaev-Landau 2 phonons $\leftrightarrow$ 1 phonon processes.

Figure 2 synthesizes our numerical results on the concavity of the bosonic branch for all values of Δ/μ and q/k_μ. Several domains can be identified depending on the values of Δ/μ, or equivalently $1/(k_Fa)$. (i) When the scattering length is negative $a<0$, that is for $\Delta/\mu<1.162$ (lower dotted line), the existence domain of the solution to Eq.(1) as a function of q is compact and simply connected [13], hence of the form $[0,q_{\mathrm{sup}}]$. The dispersion relation is entirely concave for $\Delta/\mu<0.869$ while for $0.869<\Delta/\mu<1.162$ it is first convex at small q and then concave. Between those two zones it goes through an inflection point, whose position $q_{\mathrm{infl}}(\Delta/\mu)$ we compute analytically in the small q limit [see the black dashed line and Eq.(29) of section IV]. (ii) On the other side of the resonance ($a>0$) and up to $\Delta/\mu=1.729$ (upper dotted line), the existence domain of the solution to Eq.(1) splits up into two connected components

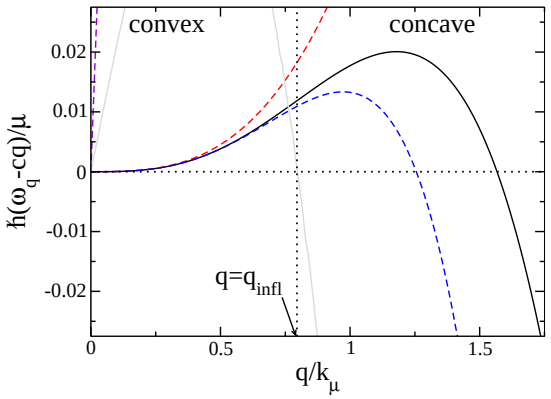

FIG. 1: (Color online) At unitarity $(k_F a)^{-1} = 0$, which is here $\Delta/\mu = 1.162$, the dispersion relation of the collective excitations is plotted as a black solid line *after subtraction* of its phononic part cq to better reveal its concavity properties. The wave number q is in units of $k_\mu = (2m\mu)^{1/2}/\hbar$. The linear part $q \mapsto cq$ is shown for comparison (steep violet dashed straight line), as well as the cubic (red dashed upper line) and the quintic (blue dashed lower line) approximations of $\omega_{\mathbf{q}} - cq$, see Eq. (10). The second order derivative $\mathrm{d}^2\omega_{\mathbf{q}}/\mathrm{d}q^2$, plotted as a gray solid line, vanishes at the inflection point $q_{\mathrm{infl}} \simeq 0.795 k_\mu$ marked by the vertical dotted line. To the left (right) of this point the dispersion relation $q \mapsto \omega_{\mathbf{q}}$ is convex (concave).

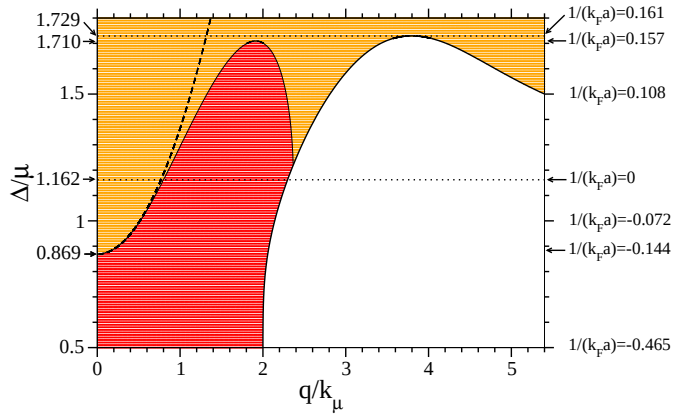

FIG. 2: (Color online) Local concavity of the bosonic branch $q \mapsto \omega_{\mathbf{q}}$ depending on Δ/μ and on the wave number q in units of $k_\mu = (2m\mu)^{1/2}/\hbar$. The values of $1/(k_F a)$ corresponding to those of Δ/μ are given on the right vertical axis. Red points show that the branch is locally concave and orange points that the branch is locally convex. The thick solid line is the border of the existence domain of the solutions of the dispersion equation (1). The black dashed line is the low-q analytical prediction (29) of the boundary between the red zone and the orange zone, that is of the locus of the inflection points of the curve $q \mapsto \omega_{\mathbf{q}}$, indicated by a thin solid line. The ordinate $\Delta/\mu = 0.869$ of the point where this line meets the $q = 0$ axis, and the ordinate $\Delta/\mu = 1.710$ above which the concavity zone disappears are indicated by arrows. For the values of Δ/μ or $1/(k_F a)$ in between the two dotted lines indicated by arrows, the q-existence domain of the solution of equation (1) is not simply connected. The lower dotted line indicates the unitary limit, where the scattering length diverges $|a| \to +\infty$.

$[0, q_{\mathrm{sup}}]$ and $[q_{\mathrm{inf}}, +\infty[$ [13]. While the branch is always convex in the second component $[q_{\mathrm{inf}}, +\infty[$, the first one $[0, q_{\mathrm{sup}}]$ exhibits interesting variations: From small q to high q, the branch is convex and then concave for $1.162 < \Delta/\mu < 1.22$, convex, concave and then convex again for $1.22 < \Delta/\mu < 1.710$ and finally entirely convex for $1.710 < \Delta/\mu < 1.729$. (iii) When Δ/μ is greater than 1.729, or negative, the two components of the existence domain merge and a solution to Eq.(1) exists for all q [13]. The branch is then entirely convex.

All these numerical values are predicted by the RPA or the BCS theory. They are therefore approximate. Up to now the only value that can be compared to experiments is that of Δ/μ at the unitary limit: From the measured values $\Delta \simeq 0.44\hbar^2 k_F^2/(2m)$ [24] and $\mu \simeq 0.376\hbar^2 k_F^2/(2m)$ [8] we get $\Delta/\mu \simeq 1.17$, which is remarkably close to the BCS-theory prediction $\Delta/\mu \simeq 1.162$. One must also keep in mind that the RPA spectrum results from a linearized treatment of the pair-field quantum fluctuations, which neglects the interactions among the bosonic quasiparticles. In reality, these interactions will shift the eigenenergies $\hbar\omega_{\mathbf{q}}$. They will also give rise, even at zero temperature, to an imaginary part in $\omega_{\mathbf{q}}$, corresponding to a finite lifetime of the excitations, provided that the concavity of the dispersion relation allows for resonant 1 phonon $\to$ 2 phonons Beliaev processes [16].

IV. ANALYTICAL STUDY OF THE CONCAVITY IN THE LONG WAVELENGTH LIMIT

The dispersion relation can be obtained analytically in the long wavelength limit $q \to 0$. To this end we expand the eigenenergy of the collective mode up to order 5 in q:

$$\hbar\omega_{\mathbf{q}} \underset{q\to 0}{=} \hbar c q \left[1 + \frac{\gamma}{8}\left(\frac{\hbar q}{mc}\right)^2 + \frac{\eta}{16}\left(\frac{\hbar q}{mc}\right)^4 + O\left(\frac{\hbar q}{mc}\right)^6\right]. \tag{10}$$

To lowest order, as for any superfluid system, the energy is phononic with a sound velocity given by the hydrodynamic expression

$$mc^2 = \rho\left(\frac{\partial\mu}{\partial\rho}\right)_a, \tag{11}$$

where the derivative is taken for a fixed scattering length a, as indicated by the notation. When applied to the approximate equation of state (9), the hydrodynamic expression (11) gives the RPA sound velocity, as shown in reference [13] by an expansion of the solution $\omega_{\mathbf{q}}$ of equation (10) up to first order in q. We give here an explicit

expression in the form of a rational fraction

$$\frac{mc^2}{\mu} = \frac{2(xy+1)}{3(y^2+1)}, \tag{12}$$

in terms of the variables

$$x = \frac{\Delta}{\mu} \quad \text{and} \quad y = \left(\frac{\partial \Delta}{\partial \mu}\right)_a . \tag{13}$$

In turn, the y variable is written as a function of x,

$$y = \frac{\int \mathrm{d}^3k \frac{\hbar^2k^2/(2m)-\mu}{\epsilon_{\mathbf{k}}^3}}{\int \mathrm{d}^3k \frac{\Delta}{\epsilon_{\mathbf{k}}^3}} = \frac{\int_0^{+\infty} \mathrm{d}u \frac{u^2(u^2-x^{-1})}{[(u^2-x^{-1})^2+1]^{3/2}}}{\int_0^{+\infty} \mathrm{d}u \frac{u^2}{[(u^2-x^{-1})^2+1]^{3/2}}} \tag{14}$$

by taking the derivative of equation (8) with respect to μ at fixed scattering length a and by expressing the wave vectors in units of $k_\Delta = (2m\Delta)^{1/2}/\hbar$ to form the dimensionless integration variable u. The integrals over u in the numerator and in the denominator of the right-hand side of equation (14) may be expressed in terms of complete elliptic integrals of the first and second kinds [11]. At the unitary limit one has $y = x$, since Δ and μ are proportional due to scale invariance.

To obtain the expression (12) of the reduced sound velocity, we take the derivative of the equation of state (9) with respect to μ at fixed a and we express all resulting integrals as functions of x and y using (14) and the relation

$$\frac{\int \frac{\mathrm{d}^3k}{(2\pi)^3} \frac{\Delta^3}{\epsilon_{\mathbf{k}}^3}}{\rho} = \frac{\int_0^{+\infty} \mathrm{d}u \frac{u^2}{[(u^2-x^{-1})^2+1]^{3/2}}}{\int_0^{+\infty} \mathrm{d}u\, u^2 \left(1 - \frac{u^2-x^{-1}}{[(u^2-x^{-1})^2+1]^{1/2}}\right)} = \frac{3x/2}{1+xy}, \tag{15}$$

which may be derived by integrating by parts the integral over u in the denominator (u^2 is the function to be integrated).

To obtain the dimensionless coefficients γ and η of the terms of $\hbar\omega_{\mathbf{q}}$ of higher order in q in equation (10), we cannot rely on known thermodynamic expressions and we must face the laborious expansion of equation (1) in powers of q. Still the result can be put into a rational form in terms of x and y:

$$\gamma = \frac{\sum_{i=0}^4 P_i(y)x^i}{135x^2\,(x^2+1)\,(y^2+1)^3}, \tag{16}$$

$$\eta = \frac{\sum_{i=0}^8 Q_i(y)x^i}{1020600\,(y^2+1)^6\,x^4\,(x^2+1)^2}. \tag{17}$$

The $P_i(y)$ and $Q_i(y)$ polynomials that appear as coefficients of x^i in the numerators of γ and η are given by

$$\begin{aligned}
P_0(y) &= -4\left(13y^4+16y^2+8\right), \\
P_1(y) &= 4y\left(13y^4+41y^2+8\right), \\
P_2(y) &= 50y^6-21y^4-252y^2-61, \\
P_3(y) &= 2y\left(y^4+32y^2+71\right), \\
P_4(y) &= 35y^6+56y^4-13y^2-54,
\end{aligned} \tag{18}$$

and by

$$\begin{aligned}
Q_0(y) &= 16\left(7745y^8+19528y^6+20304y^4+8384y^2+1088\right), \\
Q_1(y) &= 32y\left(2857y^8+67y^6-3186y^4-7920y^2-2624\right), \\
Q_2(y) &= -8\left(12882y^{10}+28061y^8-26936y^6+7221y^4-24496y^2-5232\right), \\
Q_3(y) &= -8y\left(8456y^{10}-9859y^8+9977y^6+145295y^4+3523y^2+23720\right), \\
Q_4(y) &= -17500y^{12}-247996y^{10}-1249743y^8-1341332y^6+337202y^4-694392y^2+18321, \\
Q_5(y) &= -4y\left(25564y^{10}+36027y^8-66984y^6+92206y^4+387932y^2-56121\right), \\
Q_6(y) &= -2\left(12250y^{12}+115637y^{10}+558246y^8+1071518y^6+589478y^4-248499y^2+53082\right), \\
Q_7(y) &= -4y\left(12957y^{10}+33764y^8-41904y^6-173106y^4-96189y^2+53406\right), \\
Q_8(y) &= -8575y^{12}-44544y^{10}-149742y^8-360644y^6-477615y^4-270756y^2-20412.
\end{aligned} \tag{19}$$

Our analytical expressions (16) and (17) result from a Taylor expansion of the integrals $I_{++}(\omega_{\mathbf{q}}, q)$, $I_{--}(\omega_{\mathbf{q}}, q)$ and $I_{+-}(\omega_{\mathbf{q}}, q)$ after replacement of $\hbar\omega_{\mathbf{q}}$ with the expansion (10). At each order, we reuse the results of the lower orders, that is the value (12) of c to obtain γ, and then those of c and γ (16) to obtain η. We encounter integrals involving in the denominator high powers of $\epsilon_{\mathbf{k}}$ (or of $[(u^2-x^{-1})^2+1]^{1/2}$ after the k-to-u change of variable). They can be evaluated by repeated integration by parts, as explained in Appendix A.

We have plotted in Figure 3 the coefficients γ and η as functions of the parameter $1/(k_F a)$ (which we have preferred here to Δ/μ). Let us briefly review their asymptotic behaviors in the BEC $1/(k_F a) \to +\infty$ and BCS $1/(k_F a) \to -\infty$ limits, and their values in some specific relevant regimes.

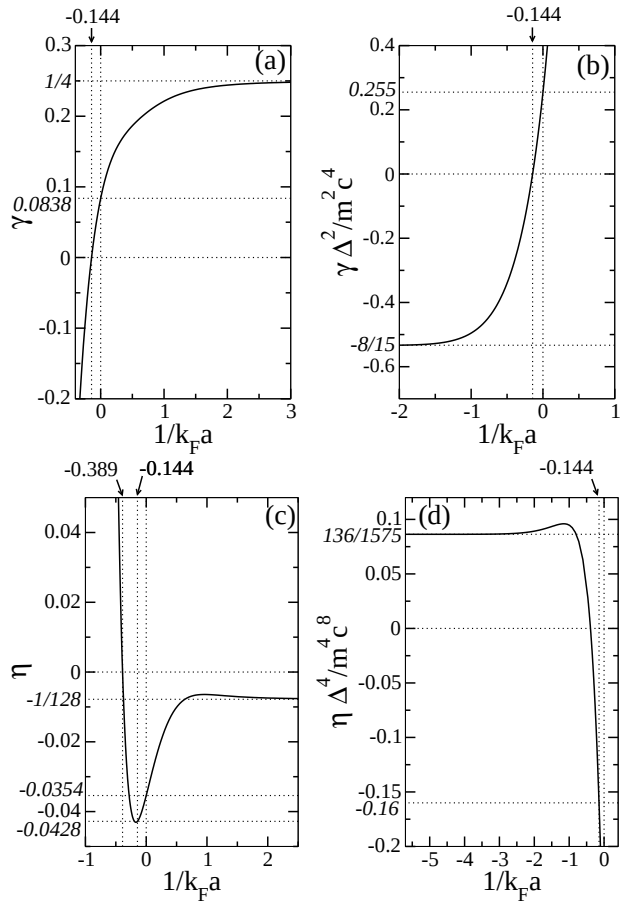

FIG. 3: Dimensionless coefficients (a) γ and (c) η of the terms q^3 and q^5 in the RPA dispersion relation of the bosonic excitations for $q \to 0$, see equation (10), as functions of the interaction parameter $1/(k_F a)$. In the BEC limit, they have a finite limit corresponding to the Bogoliubov dispersion relation, see equations (21,22). In the BCS limit, they diverge, and it is more appropriate to express the wave number q in units of $\Delta/(\hbar c)$, which amounts to considering the quantities (b) $\gamma\Delta^2/(m^2c^4)$ and (d) $\eta\Delta^4/(m^4c^8)$ which have a finite limit. In between these two limits, γ and η vanish and change sign for $1/(k_F a) \simeq -0.144$ and $1/(k_F a) \simeq -0.389$ respectively, and they are weakly positive ($\gamma \simeq 0.0838$) or weakly negative ($\eta \simeq -0.0354$) at the unitary limit. The value of η is relevant mainly at the point where γ vanishes. At this point, $\eta \simeq -0.0428$ so the RPA dispersion relation is concave over a neighborhood of $q = 0$.

1. BEC limit

In the BEC limit $k_F a \to 0^+$, the system is equivalent to a weakly interacting gas of bosons of mass $2m$, with a chemical potential

$$\mu_B = 2\mu - E_{\rm dim}, \tag{20}$$

where $E_{\rm dim} = -\hbar^2/(ma^2)$ is the internal energy of a dimer [25, 26]. The dispersion relation of the bosonic excitations is then known to be convex and to take the Bogoliubov form at chemical potential μ_B when $q = o(1/a)$ [13]:

$$\hbar\omega_{\mathbf{q}}^{\rm Bog} = \left[\frac{\hbar^2 q^2}{4m}\left(\frac{\hbar^2 q^2}{4m} + 2\mu_B\right)\right]^{1/2}, \tag{21}$$

in which case the sound velocity is given by $2mc^2 = \mu_B$. The coefficients γ and η are thus expected to have the following limits:

$$\gamma \underset{k_F a \to 0^+}{\to} \frac{1}{4} \quad \text{and} \quad \eta \underset{k_F a \to 0^+}{\to} -\frac{1}{128}. \tag{22}$$

This is confirmed by equations (16) and (17) taken at the BEC limit, that is for $x = O(k_F a)^{3/2} \to 0^-$ [22] and, as shown by equation (14) after the change of variable $u = u'/|x|^{1/2}$, for $y \sim -4/x$.

2. BCS limit

When $k_F a \to 0^-$, the lower border of the two-fermionic-excitation continuum (at fixed total wave number $q < q_{\rm sup}$) becomes exponentially weak and forces the bosonic excitation branch, which cannot enter into this continuum, to bend downward [13, 15]. This bending takes place over a wave number range q_c such that $\hbar c q_c = \Delta$, that is such that the leading term in the expansion (10) is of the order of Δ. This means that the collective modes are affected by the pairs internal structure when the mode wavelength becomes comparable to the pairs size in real space $\approx \hbar^2 k_F/(m\Delta)$ [11], a quantity that is indeed of order $1/q_c$ since $c \propto \hbar k_F/m$ in the BCS limit. This qualitatively explains why the dispersion relation is a concave function of q for low q and low Δ/μ in Figure 2, and why $\gamma < 0$ in the BCS limit.

More quantitatively, we expect that the normalized energy $\hbar\omega_{\mathbf{q}}/\Delta$ becomes a universal function of $q/q_c = \hbar c q/\Delta$ when $k_F a \to 0^-$, in which case all the terms in square brackets in equation (10) are of the same order of magnitude for $q = q_c$, that is $|\gamma(\hbar q_c/mc)^2| \approx 1$, $|\eta(\hbar q_c/mc)^4| \approx 1$. This is indeed what we find by taking the limits $x \to 0$ and $y \to 0$ in equations (16) and (17):

$$\gamma \underset{k_F a \to 0^-}{\sim} -\frac{8}{15}\left(\frac{mc^2}{\Delta}\right)^2 \quad \text{and} \quad \eta \underset{k_F a \to 0^-}{\sim} \frac{136}{1575}\left(\frac{mc^2}{\Delta}\right)^4, \tag{23}$$

the first result reproducing that of reference [11].

3. Crossover region

In the crossover region between BEC and BCS, γ is an increasing function of $1/(k_F a)$. It vanishes and changes sign for the value x_0 of $x = \Delta/\mu$ given by

$$x_0 \simeq 0.868567. \tag{24}$$

This value corresponds to $1/(k_F a) \simeq -0.144292$, in agreement with the numerical result of Figure 2 and with reference [16]. The RPA prediction is then that the dispersion relation of a unitary gas is convex close to $q = 0$:

$$\gamma \underset{(k_F a)^{-1}=0}{\simeq} 0.083769. \tag{25}$$

The coefficient η changes sign for a value x_1 of Δ/μ given by

$$x_1 \simeq 0.566411 \tag{26}$$

corresponding to $1/(k_F a) \simeq -0.389027$. It is negative both at unitarity

$$\eta \underset{(k_F a)^{-1}=0}{\simeq} -0.035416, \tag{27}$$

and at the point x_0 where $\gamma = 0$:

$$\eta(x_0) \simeq -0.042794. \tag{28}$$

At that very point the sign of η is important as it determines the concavity of the dispersion relation close to $q = 0$.

4. Locus of the inflection points

The coefficients γ and η allow us to find analytically the border between the orange and the red zones of Figure 2 for small q, that is the ensemble of points with coordinates $(q_{\rm infl}/k_\mu, \Delta/\mu)$ such that the second derivative $\mathrm{d}^2\omega_{\mathbf{q}}/\mathrm{d}q^2$ is zero. Using the expansion (10) for $\omega_{\mathbf{q}}$ and expanding the coefficients $\gamma(x)$ and $\eta(x)$ around $x = x_0$, to order one and order zero in $x - x_0$ respectively, one obtains the equation

$$\frac{q_{\rm infl}^2}{k_\mu^2} \underset{x\to x_0^+}{\sim} -\frac{3\gamma'(x_0)}{10\eta(x_0)}\frac{mc^2}{\mu}(x - x_0) \simeq 2.015858(x - x_0) \tag{29}$$

plotted as a black dashed curve in Figure 2, which reaches the axis $q = 0$ with a horizontal tangent.

In contrast, the border between the red and orange zones in Figure 2 reaches the border of the existence domain of the collective excitation branch with an oblique tangent. This is due to the fact that the third derivative of $q \mapsto \omega_{\mathbf{q}}$ is nonzero at the contact point $q = q_{\rm sup}$ contrarily to what happens at $q = 0$.

V. CONCLUSION

We have considered a spatially homogeneous unpolarized gas of spin-1/2 fermions at zero temperature, and we have obtained analytically the spectrum $\hbar\omega_{\mathbf{q}}$ of the bosonic excitation branch predicted by the RPA up to order 5 included in the wave vector q close to $q = 0$. The coefficients of the obtained expansion are rational fractions of two variables Δ/μ and $(\partial\Delta/\partial\mu)_a$, where the second variable can be analytically related to the first one using the BCS equation of state. This allows us to show analytically that the dispersion relation $q \mapsto \omega_{\mathbf{q}}$ is concave close to $q = 0$ when $1/(k_F a)$ is between $-\infty$ and a value close to -0.144, a point where the first correction to the linear dispersion relation is of order q^5 with a slightly negative coefficient. For $-0.144 < 1/(k_F a) < 0.157$ the branch is convex close to $q = 0$ but becomes concave when q increases, and it remains so for q increasing up to the maximal possible value $q_{\rm sup}$ if $1/(k_F a) < 0.022$, while it becomes convex again in the opposite case $0.022 < 1/(k_F a) < 0.157$. Beyond $1/(k_F a) = 0.157$ the bosonic branch is convex over its whole existence domain.

A straightforward application of our quintic approximation (10) for the spectrum is to determine if a low-q collective excitation of the Fermi gas can decay *via* a Beliaev process, that is into two collective excitations of wave vectors $\mathbf{q}_1$ and $\mathbf{q}_2 = \mathbf{q} - \mathbf{q}_1$. Energy conservation allows such a process if $\omega_{\mathbf{q}} > \Omega_{\mathbf{q}}^{\rm inf}$ where $\Omega_{\mathbf{q}}^{\rm inf} = \inf_{\mathbf{q}_1}(\omega_{\mathbf{q}_1} + \omega_{\mathbf{q}-\mathbf{q}_1})$ is the lower border of the two-excitation continuum at fixed total wave vector $\mathbf{q}$. If Δ/μ is away from the critical value $x_0 \simeq 0.869$ where the coefficient γ of q^3 vanishes, the dispersion relation is either entirely convex or entirely concave at low q, and the Beliaev decay is respectively allowed or forbidden. If Δ/μ is close to the critical value x_0, the dispersion relation has an inflection point at low q. We then apply the analysis of reference [15] to Eq. (10) and we find $\Omega_{\mathbf{q}}^{\rm inf} = \min(2\omega_{\mathbf{q}/2}, \omega_{\mathbf{q}})$ [32]. The Beliaev decay is thus allowed if

$$\left(\frac{\hbar q}{mc}\right)^2 < \frac{8\gamma}{5|\eta|} \tag{30}$$

to leading order in γ, that is in $\Delta/\mu - x_0$. At low but nonzero temperature, there exist additional decay mechanisms: (i) The Landau mechanism $\mathbf{q}+\mathbf{q}_1 \to \mathbf{q}_2$ is forbidden whenever the Beliaev one is since it can be viewed as an inverse Beliaev mechanism with an initial wave vector $\mathbf{q}_2$ of modulus $> q$; (ii) the higher-order Landau-Khalatnikov decay process $\mathbf{q} + \mathbf{q}_1 \to \mathbf{q}_2 + \mathbf{q}_3$ is always allowed, but it is subleading when the Beliaev or Landau processes are present.

Our results on the concavity of the dispersion relation close to $q = 0$ can be tested experimentally in a gas of cold atoms trapped in a flat bottom potential [27]. This can be done either (i) indirectly by measuring dissipative effects such as the damping of collective excitations at low

temperature, or dispersive effects such as the spreading of a wave packet of sound waves created by a laser pulse [9, 28], or (ii) directly by accessing the dispersion relation at low temperature *via* the dynamic structure factor of the Fermi gas through Bragg excitation at a selected wave vector $\mathbf{q}$ [29–31] [33]. Supplemented by kinetic equations for the collective mode occupation numbers, our results open the way to an analytical determination of the phase diffusion coefficient at low temperature, hence to the intrinsic limit to the coherence time of the condensate of pairs in a finite-size Fermi gas [14].

Appendix A: Expressing integrals in terms of the variables x and y

In the expansion of $I_{++}(\omega_{\mathbf{q}}, q)$, $I_{--}(\omega_{\mathbf{q}}, q)$ and $I_{+-}(\omega_{\mathbf{q}}, q)$ at low q, and after a rescaling of the wave vectors by k_Δ as in equation (14), $k = uk_\Delta$, we encounter integrals of the form

$$I_{n,p} = \frac{k_\Delta^3}{2\pi^2\rho}\int_0^{+\infty} \mathrm{d}u \frac{u^{2p+2}}{\epsilon_u^n}, \tag{A1}$$

$$J_{n,p} = \frac{k_\Delta^3}{2\pi^2\rho}\int_0^{+\infty} \mathrm{d}u \frac{u^{2p+2}\xi_u}{\epsilon_u^n} \tag{A2}$$

with $n \in 2\mathbb{N}^* + 1$, $p \in \mathbb{N}$,

$$\xi_u = u^2 - \frac{1}{x}, \tag{A3}$$

$$\epsilon_u = \sqrt{\xi_u^2 + 1}, \tag{A4}$$

and the total density ρ is given by equation (9). The integrals giving $I_{n,p}$ and $J_{n,p}$ are convergent for $n-p \geq 2$ and for $n-p \geq 3$, respectively. Integrals that depend on the direction of $\mathbf{k}$ can be expressed in the forms (A1) and (A2) after angular integration:

$$\int \mathrm{d}^3k f(k) \left(\frac{\hbar^2 \mathbf{k}\cdot\mathbf{q}}{m}\right)^{2p} = \frac{4\pi}{1+2p}\left(\frac{\hbar^2 q^2}{m}\right)^p \int_0^{+\infty} \mathrm{d}k k^2 f(k) \left(\frac{\hbar^2 k^2}{m}\right)^p \tag{A5}$$

where $f(k)$ is an arbitrary function of the modulus of $\mathbf{k}$.

Let us first establish the four recurrence relations

$$I_{n,p} = \frac{n-3}{n-2} I_{n-2,p} - \frac{2p+1}{2(n-2)} J_{n-2,p-1}, \tag{A6}$$

$$J_{n,p} = \frac{2p+1}{2(n-2)} I_{n-2,p-1}, \tag{A7}$$

$$I_{n,p} = J_{n,p-1} + \frac{I_{n,p-1}}{x}, \tag{A8}$$

$$J_{n,p} = \frac{J_{n,p-1}}{x} + I_{n-2,p-1} - I_{n,p-1}, \tag{A9}$$

holding under the conditions $1 \leq p \leq n-4$ for the first relation, $1 \leq p \leq n-3$ for the second one, $1 \leq p \leq n-2$ for the third one and $1 \leq p \leq n-3$ for the last one. In order to derive the relation (A6), we integrate by parts the integral

$$\frac{k_\Delta^3}{2\pi^2\rho}\int_0^{+\infty} \mathrm{d}u \frac{u^{2p+2}\xi_u^2}{\epsilon_u^n} = I_{n-2,p} - I_{n,p}, \tag{A10}$$

selecting $u \mapsto u^{2p+1}\xi_u$ as the function to be differentiated. In order to derive the relation (A7), we integrate by parts the integral defining $J_{n,p}$ in equation (A2), selecting $u \mapsto u^{2p+1}$ as the function to be differentiated. In both cases, we note that the function $u \mapsto u\xi_u/\epsilon_u^n$ admits the primitive $u \mapsto -[2(n-2)\epsilon_u^{n-2}]^{-1}$. Finally, we simply write $u^{2p+2} = u^{2p}(\xi_u + x^{-1})$ in the integrand of (A1) in order to obtain (A8), and we write $u^{2p+2}\xi_u = u^{2p}(\epsilon_u^2 - 1 + x^{-1}\xi_u)$ in the integrand of (A2) in order to obtain (A9). This procedure generalizes that of reference [11].

We now show by induction using the relations (A6,A7,A8,A9) that $I_{n,p}$ and $J_{n,p}$ can be expressed as functions of $I_{3,0}$ and $J_{3,0}$, for all odd $n \geq 3$ and for all positive p within the existence domain of the integrals. Let n be odd and ≥ 3 and assume that we know all the $I_{n,p}$, $0 \leq p \leq n-2$, and all the $J_{n,p}$, $0 \leq p \leq n-3$. Then (i) $I_{n+2,1}$ and $J_{n+2,1}$ can be deduced using (A6) and (A7), (ii) using (A9) and (A8) we obtain a Cramer system for $I_{n+2,0}$ and $J_{n+2,0}$:

$$x^{-1}J_{n+2,0} - I_{n+2,0} = J_{n+2,1} - I_{n,0}, \tag{A11}$$

$$J_{n+2,0} + x^{-1}I_{n+2,0} = I_{n+2,1}, \tag{A12}$$

which we solve, (iii) we use (A8) and (A9) to access the values of $I_{n+2,p}$ and $J_{n+2,p}$ for $p \geq 2$. We set the induction basis at $n = 3$, by expressing $I_{3,1}$ as a function of $I_{3,0}$ and $J_{3,0}$ due to (A8).

Finally we relate $I_{3,0}$ and $J_{3,0}$ to x and y thanks to the relations (14) and (15) of the main text, which take the form $y = J_{3,0}/I_{3,0}$ and $I_{3,0} = 3x/[2(1+xy)]$ with the notation of this appendix.

[1] K. M. O'Hara, S. L. Hemmer, M. E. Gehm, S. R. Granade, and J. E. Thomas, Science **298**, 2179 (2002).
[2] T. Bourdel, J. Cubizolles, L. Khaykovich, K. M. F. Magalhães, S. J. J. M. F. Kokkelmans, G. V. Shlyapnikov, and C. Salomon, Phys. Rev. Lett. **91**, 020402 (2003).
[3] M. Bartenstein, A. Altmeyer, S. Riedl, S. Jochim, C. Chin, J. Hecker Denschlag, and R. Grimm, Phys. Rev. Lett. **92**, 120401 (2004).
[4] M. Bartenstein, A. Altmeyer, S. Riedl, S. Jochim, C. Chin, J. Hecker Denschlag, and R. Grimm, Phys. Rev. Lett. **92**, 203201 (2004).
[5] M. W. Zwierlein, C. A. Stan, C. H. Schunck, S. M. F. Raupach, A. J. Kerman, and W. Ketterle, Phys. Rev. Lett. **92**, 120403 (2004).
[6] M. W. Zwierlein, J. R. Abo-Shaeer, A. Schirotzek, C. H. Schunck, and W. Ketterle, Nature **435**, 1047 (2005).
[7] S. Nascimbène, N. Navon, K. J. Jiang, F. Chevy, and C. Salomon, Nature **463**, 1057 (2010).
[8] M. J. H. Ku, A. T. Sommer, L. W. Cheuk, and M. W. Zwierlein, Science **335**, 563 (2012).
[9] L. A. Sidorenkov, M. K. Tey, R. Grimm, Y.-H. Hou, L. Pitaevskii, and S. Stringari, Nature **498**, 78 (2013).
[10] P. Anderson, Phys. Rev. **112**, 1900 (1958).
[11] M. Marini, F. Pistolesi, and G. Strinati, Eur. Phys. J. B **1**, 151 (1998).
[12] M. Randeria and E. Taylor, Annu. Rev. Condens. Matter Phys. **5**, 209 (2014).
[13] R. Combescot, M. Y. Kagan, and S. Stringari, Phys. Rev. A **74**, 042717 (2006).
[14] H. Kurkjian, Y. Castin, and A. Sinatra, arXiv:1502.05644 & hal-01118346 (2015).
[15] Y. Castin, I. Ferrier-Barbut, and C. Salomon, C. R. Physique **16**, 241 (2015).
[16] G. Bighin, L. Salasnich, P. A. Marchetti, and F. Toigo, Phys. Rev. A **92**, 023638 (2015).
[17] S. Beliaev, Zh. Eksp. Teor. Fiz. **34**, 417 (1958).
[18] P. O. Fedichev and G. V. Shlyapnikov, Phys. Rev. A **58**, 3146 (1998).
[19] L. Landau and I. Khalatnikov, Zh. Eksp. Teor. Fiz. **19**, 637 (1949).
[20] Z. Zhang and W. V. Liu, Phys. Rev. A **83**, 023617 (2011).
[21] J. Bardeen, L. Cooper, and J. Schrieffer, Phys. Rev. **108**, 1175 (1957).
[22] Y. Castin, in *Ultra-cold Fermi Gases*, edited by M. Inguscio, W.Ketterle, and C. Salomon (Società italiana di fisica, Bologna, Italia, 2007).
[23] H. Kurkjian, Y. Castin, and A. Sinatra, Phys. Rev. A **88**, 063623 (2013).
[24] A. Schirotzek, Yong-il Shin, C. H. Schunck, and W. Ketterle, Phys. Rev. Lett. **101**, 140403 (2008).
[25] X. Leyronas and R. Combescot, Phys. Rev. Lett. **99**, 170402 (2007).
[26] R. Combescot and X. Leyronas, Phys. Rev. A **78**, 053621 (2008).
[27] A. L. Gaunt, T. F. Schmidutz, I. Gotlibovych, R. P. Smith, and Z. Hadzibabic, Phys. Rev. Lett. **110**, 200406 (2013).
[28] M. R. Andrews, D. M. Kurn, H.-J. Miesner, D. S. Durfee, C. G. Townsend, S. Inouye, and W. Ketterle, Phys. Rev. Lett. **79**, 553 (1997).
[29] J. Stenger, S. Inouye, A. P. Chikkatur, D. M. Stamper-Kurn, D. E. Pritchard, and W. Ketterle, Phys. Rev. Lett. **82**, 4569 (1999).
[30] J. Steinhauer, R. Ozeri, N. Katz, and N. Davidson, Phys. Rev. Lett. **88**, 120407 (2002).
[31] E. D. Kuhnle, H. Hu, X.-J. Liu, P. Dyke, M. Mark, P. D. Drummond, P. Hannaford, and C. J. Vale, Phys. Rev. Lett. **105**, 070402 (2010).
[32] Since the dispersion relation $q \mapsto \omega_{\mathbf{q}}$ is here an increasing function, only the cases (i) and (ii) of Eq. (12) in reference [15], where $\mathbf{q}_1$ and $\mathbf{q}-\mathbf{q}_1$ have the same direction at the minimum of $\omega_{\mathbf{q}_1}+\omega_{\mathbf{q}-\mathbf{q}_1}$, need to be considered. It remains to minimize the function $f(q_1)=\omega(q_1)+\omega(q-q_1)$ over the interval $[0,q/2]$, where $\omega(q)=\omega_{\mathbf{q}}$ is given by Eq. (10). Using the parametrization $q_1=(1-t)q/2$, with $t\in[0,1]$, we find that $f(q_1)$ is a concave parabolic function of t^2. The minimum of $f(q_1)$ is thus reached at the border of the interval and is either $f(0)=\omega_{\mathbf{q}}$ or $f(q/2)=2\omega_{\mathbf{q}/2}$.
[33] In reference [30] the spectrum is measured with an uncertainty ± 18Hz at low q. For the typical Fermi temperature $T_F=1\mu$K, this corresponds to an uncertainty $\pm 2\times 10^{-3}$ on $\hbar\omega_{\mathbf{q}}/\mu$ that is on the vertical axis of Figure 1, indicating that the convexity of $q\mapsto\omega_{\mathbf{q}}$ is experimentally determinable for the unitary Fermi gas.